Published by
NIGERIAN SOCIETY OF PHYSICAL SCIENCES
Available online @ https://journal.nsps.org.ng/index.php/jnsps

J. Nig. Soc. Phys. Sci. 6 (2024) 2203

Journal of the Nigerian Society of Physical Sciences

Synthesis and characterization of MnO_2 nanoparticles mediated by *Raphia hookeri* seed

Bamidele H. Akpeji[a,b,*], Bulouebibo Lari[c], Ufuoma A. Igbuku[d], Godswill O. Tesi[e], Elias E. Elemike[b,e], Paul O. Akusu[f]

[a]*Department of Science Laboratory Technology, Federal University of Petroleum Resources, P.M.B 1221, Effurun, Delta State, Nigeria*
[b]*Centre for Sustainable Development, Federal University of Petroleum Resources, P.M.B 1221, Effurun, Delta State, Nigeria*
[c]*Department of Science Laboratory Technology, Delta State University, Abraka, Delta State, Nigeria*
[d]*Department of Chemistry, Delta State University of Science and Technology, Ozoro, Delta State, Nigeria*
[e]*Department of Chemistry, Federal University of Petroleum Resources, P.M.B 1221, Effurun, Delta State, Nigeria*
[f]*Department of Petroleum and Natural Gas Processing, Petroleum Training Institute, Effurun, Delta State, Nigeria*

Abstract

In this study, manganese dioxide nanoparticles (MnO_2NP) was biosynthesized. *Raphia hookeri* seed was used as a bioreductant for the synthesis of MnO_2NPs using bottom up approach. The biosynthesized MnO_2NPs was investigated for their reaction, structure and morphology. The MnO_2NPs was characterized using the UV-Visible spectrophotometry, Fourier Transform Infrared Spectrophotometry (FTIR), Energy Dispersive Spectrometry (EDX), Powdered X-ray Diffractometry (PXRD), Scanning electron microscpopy (SEM) and Transmission Electron Microscopy (TEM). UV-Visible spectrum revealed that MnO_2NPs showed maximum absorption at wavelength of 421nm in the visible region. FTIR results showed prominent reactive functional groups for hydroxyl (-OH) at 3348.30 cm^{-1} and a weak carbonyl (-C=O) at 1700.00 cm^{-1} . The EDX results revealed the elemental composition in percentages of the elements in the nanoparticles, showing Mn (70.96 %), O (25.67 %) and C (8.34%) respectively. PXRD revealed that the manganese dioxide nanoparticle is in a crystalline state. The morphology of the synthesized nanoparticle was found irregular and with porous surface for SEM. The average particle size of the nanoparticles as characterized by TEM was found to be 3.92 nm.

DOI:10.46481/jnsps.2024.2203

Keywords: Synthesis, Characterization, Nanoparticles, MnO_2NP, *Raphia hookeri* seed

Article History :
Received: 19 June 2024
Received in revised form: 14 July 2024
Accepted for publication: 09 August 2024
Published: 08 September 2024

Communicated by: Emmanuel Etim

1. Introduction

Nanotechnology is now a promising area with potential uses in electronics, medicine, energy, and environment [1, 2]. Among the most studied nanoparticles, manganese dioxide nanoparticles (MnO_2NPs) are found to possess remarkable characteristics and multiple applications. Brindhadevi *et al.* [3] proffered that chemically synthesized MnO_2 nanoparticles has been previously developed by several techniques such as chemical, physical and biological method, all embedded in top-up and bottom-up approaches. Of these, the use of biological species,

*Corresponding Author Tel. No.: +234-806-017-4341.
Email address: akpeji.honesty@fupre.edu.ng (Bamidele H. Akpeji)

for instance, plant extracts which are ecofriendly and relatively cheap represents a plausible approach toward obtaining green synthesis of nanomaterials [4]. The green synthesis approach including plant extracts as reducing and capping agents is advantageous compared to the conventionally adopted chemical route as stated by Penghui & Hengyi [5]. First of all, it does not involve the usage of toxic compounds, which reduces the extent of toxicity as a threat to the environment and people's health and guarantees compatibility with the organism in case of using the nanocomposite for biomedical purposes. Second, due to the presence of phytochemicals that exists in the plant extract, reduction of metal ions and stability of nanoparticles becomes easier and the nanoparticles formed possess better defined morphology and stability. Thirdly, the synthesis process is easy to perform, economically cheap, and scalable for the large scale production which makes it industrial relevant [4, 6–10].

Raphia hookeri is a palm species that is found in West African region and due to its multi-utility in terms of pharmacological and biological activities and has several uses in traditional medicine while the stalk is utilized in ornaments and to build mats and baskets. The seed of *Raphia hookeri* is locally called "Oje" or "Ozi" among the Igbos, "Oroke" or "Oroko" among the Yorubas, whereas the Hausa people of Nigeria knew it as "Kantaka" or "Kanta". Meanwhile, it is commonly known as Raphia palm seed in English. *Raphia hookeri* seed is a waste material whose potential in the synthesis of MnO_2NPs is investigated in this study.

Raphia hookeri seeds contain phytochemicals including phenolics, terpenoids, flavonoids, and reducing sugars, which introduced the seeds as favourable material for controlling the formation of metallic nanoparticles Mohammad *et al.* [11].

This paper aims at the synthesis and characterization of MnO_2 nanoparticles prepared from extract of *Raphia hookeri* seed (R.H.S). This work on MnO_2 using seeds of *Raphia hookeri* suggests the discovery of a new way of synthesizing MnO_2NPs using different precursor concentration, and green synthesis as well. This study integrates biocompatibility and eco-friendliness by making use of the seeds of *Raphia hookeri*, a West African palm into the synthesis of manganese dioxide nanoparticles (MnO_2NPs). Besides, offering an ecofriendly method in place of chemical synthesis approaches, this method also touches on the prospects of MnO_2NPs produced by biological methods as well as their special characteristics.

2. Materials and method

2.1. Materials

Chemicals and reagents like sodium hydroxide (NaOH), manganese acetate dihydrate [$Mn(CH_3COO)_2$. $2H_2O$], Chloroform ($CHCl_3$), aqueous ammonia [$NH_{3(aq)}$], Mayer's reagent, concentrated sulpuric acid (H_2SO_4), concentrated nitric acid (HNO_3), ferric chloride ($FeCl_3$), Fehling's solution, Buiret's solution, Tollen's reagent are of analytical grade obtained from Sigma Aldrich Chemicals. Distilled water was gotten from Chemistry Laboratory, Federal University of Petroleum Resources, Delta State, Nigeria.

2.2. Method

2.2.1. Collection, extraction and phytochemical screening of Raphia hookeri Seed

The *Raphia hookeri* seed was plucked from its cub located at Toru Ndoro community of Bayelsa State and was identified in the department of botany in University of Benin. The extraction and phytochemical screening was performed in accordance with the procedures laid out by Oluyori [12] and Okewale and Akpeji [13] with slight variation in the procedure applied. In this work, apparatus was assembled, round-bottom flask conduit to the condenser and thimble with 100 g of powdered *Raphia hookeri* seed was measured and placed in a round bottom flask. Water was chosen as the solvent due to its potent capacity of extracting a series range of phytochemicals from plant tissues. Vaporization in the round-bottom flask was achieved utilising a heating mantle, allowing water to be converted into its gaseous form and then re-liquefied onto cooling down within condenser. This cycle of process allowed for the *Raphia hookeri* seed to be continuously extracted over a period that was extended in time, generally for 4 hours. Cold condition was maintained on the condenser throughout the extraction period for exhaustive removal of bioactive constituents. When the extraction was considered finished, aqueous extract with phytochemicals solublized in it was sedimented by slow heating at controlled temperature of 70 °C. This process would allow the good reduction of the water to obtain a concentrated *Raphia hookeri* extracts for phytochemical analysis.

Test for alkaloids: To about 0.5 g of the aqueous extract *Raphia hookeri*, two drops of Mayer's reagent were added along the sides of test tube. Appearance of white creamy precipitate was observed which indicated the presence of alkaloids.

Test for reducing sugar: To about 0.5 g of the aqueous extract in the test tube, tollen's reagent was added and heated moderately. The presence of silver mirror on the walls of the test tube indicates the presence of reducing sugars.

Test for steroids: 0.5 g of the aqueous extracts was taken in a test tube and dissolved with chloroform (10 mL), then three drops of concentrated sulphuric acid was added by the side of the test tube. Result showed negative to steroids. Positive result should give two layers. The upper layer should give red and sulphuric acid layer should give yellow with green fluorescence.

Test for terpenoids: 0.5 g of extract was mixed in 2 mL of chloroform and 3 mL of concentrated H_2S0_4 was carefully added to form a layer. A reddish brown colouration of the inter face indicate the presence of terpenoids. Meanwhile, in this work, it was found negative.

Test for saponin: To about 0.5 g of the aqueous extract in the testube was added 5 mL of distilled water. It was shaken vigourously. Persistent foam for about 2 minutes confirmed the presence of saponin.

Test for anthraquinones: 0.5 g of the aqueous extract was boiled with 1 mL concentrated HNO_3 and shaken well. A dark orange colour indicates the presence of anthraquinones on addition of the concentrated acid. Meanwhile, in this work, result obtained showed negative.

Test for phenolic compounds: To 0.5 g of the aqueous extract,

few drops of 10% ferric chloride solution was added. Green blue colour appears which indicated the presence of phenolic compounds.

Test for carbohydrates: 5 mL of Fehling's solution was added to 0.5 g of the aqueous extract and heated in a water bath. The formation of yellow precipitate was observed which indicated the presence of carbohydrate.

Test for tannins: About 0.5 g of the aqueous extract, 5% ferric chloride solution was added, a dark green precipitate was observed which showed the presence of tannins in the plant.

Test for flavonoids: To 0.5 g of aqueous extract was added little quantity of water. A few drop of lead acetate solution was added and a light yellow precipitate was observed which indicated the presence of flavonoid.

2.2.2. *Bio-synthesis of manganese dioxide nanoparticles from Raphia hookeri seed*

The synthesis processes is similar to those of Haibin *et al.* [14], Brindhadevi *et al.*[3], and Abelneh [4], with a minor modifications. In this synthesis, the *Raphia hookeri* seed was plucked from its cub and washed with distilled water. It was then airdried for 7 days and pulverized to power using a local machine grinder in the market. 2g of the pulverized R.H.S was measured into a clean conical flask and 200 mL of distilled water was added. The content was heated on the heating mantle for 2 hrs and filtered to make an aqueous extract. 25 mL of the aqueous *Raphia hookeri* seed extract and 500 mL of the 0.02M manganese acetate solution were combined at a ratio of 1:20, and 30 mL of NaOH solution was added gradually. Using a magnetic stirrer, the resultant liquid was then fully mixed by swirling continuously for around three hours at 70° C. The solution's colour steadily transformed from brown to black throughout the reaction period, suggesting a rate of bio-reduction of the manganese acetate and the precipitation of manganese hydroxide $Mn(OH)_2$. The precipitate was centrifuged and the black residue obtained was dried in a LD-201-E Vision Scientific drying oven at 70^oC. A UV-Vis spectrophotometer was used to observed the formation of manganese dioxide nanoparticles after the fluid underwent further churning on the magnetic stirrer. The synthetic process could be seen to occur in equation 1:

$$[Mn(CH_3COO)_2.2H_2O]+(Phyto-enzymes\ \ from\ \ R.H.S)+ NaOH \rightarrow Mn(OH)_2+drying\ \ to\ \ removeH_2O \rightarrow MnO-NP \quad (1)$$

2.2.3. *Instrumental characterization of the MnO_2NPs*

The formation of the MnO_2 nanoparticles was determined using Perkin Elmer Lambda 40 UV-visible spectrometer. Model Nicolet iS10 FT-IR Spectrometer was used for the analysis of the reactivity and functional groups present in the synthesized MnO_2 nanoparticles. The scanning electron microscope (SEM) of model JOEL JSM-IT71OHR-BECTHAI is a highly specialized instrument that captured shape of the biosynthesized MnO_2 nanoparticles by utilizing a focused electron beam to scan its surface. The elemental composition of the nanomaterials were checked for using EDX-8100 model. The morphology and particle size of the nanoparticles were determined using JEM-ARM200F-G-TEM instrument whereas the crystallinity of the materials was determined with the aid of Rigaku D/Max-IIIC X-ray diffractometer.

Table 1. Phytochemical analysis of aqueous extract *Raphia hookeri* seed.

Test performed	Results
Appearance	Liquid
Colour Description	brown
Saponin	+
Reducing Sugar	+
Alkaloids	+
Steroids	-
Tannins	+
Anthraquinones	-
Phenolic compounds	+
Carbohydrates	+
Terpenoids	-
Flavonoids	+

Keys; (+) detected, (-) Not detected

3. Results and discussion

3.1. *Phytochemical characterization of aqueous plant extract of Raphia hookeri seed*

The result of the phytochemical experiment on the aqueous extract of *Raphia hookeri* seed extract reveals the presence of some phytochemicals is presented in Table 1.

The result of the phytochemical analysis on *Raphia hookeri* seed is given in Table 1. Result showed that the presence of saponins, alkaloids, tannis, phenolic compounds, carbohydrates, glycosides, flavonoids and reducing sugar which may be responsible for the reduction of manganese acetate dihydrate into manganese dioxide. It is believed that the plant extract has information to give in the bio-reduction of the metal precursor in the synthesis of nano-metal particles [12]. Similar result was obtained in the findings of Samy *et al.* [15] on the phytochemical characterization of *Raphia hookeri* seed extract.

3.2. *Characterization of nanoparticles*

Any synthesis process must start with an understanding of the final product's composition or structure. To do this, a variety of techniques may be applied, such as deciphering the structure to determine the concentration and level of purity of the synthesized materials. To address the question of whether nanoparticles was produced using this process, the synthesized MnO_2NPs would be subjected to analysis using UV-Visible spectrophotometry, FTIR, SEM, TEM, EDX, and PXRD. These techniques can yield valuable insights into the chemistry of the biosynthesized MnO_2 nanoparticle.

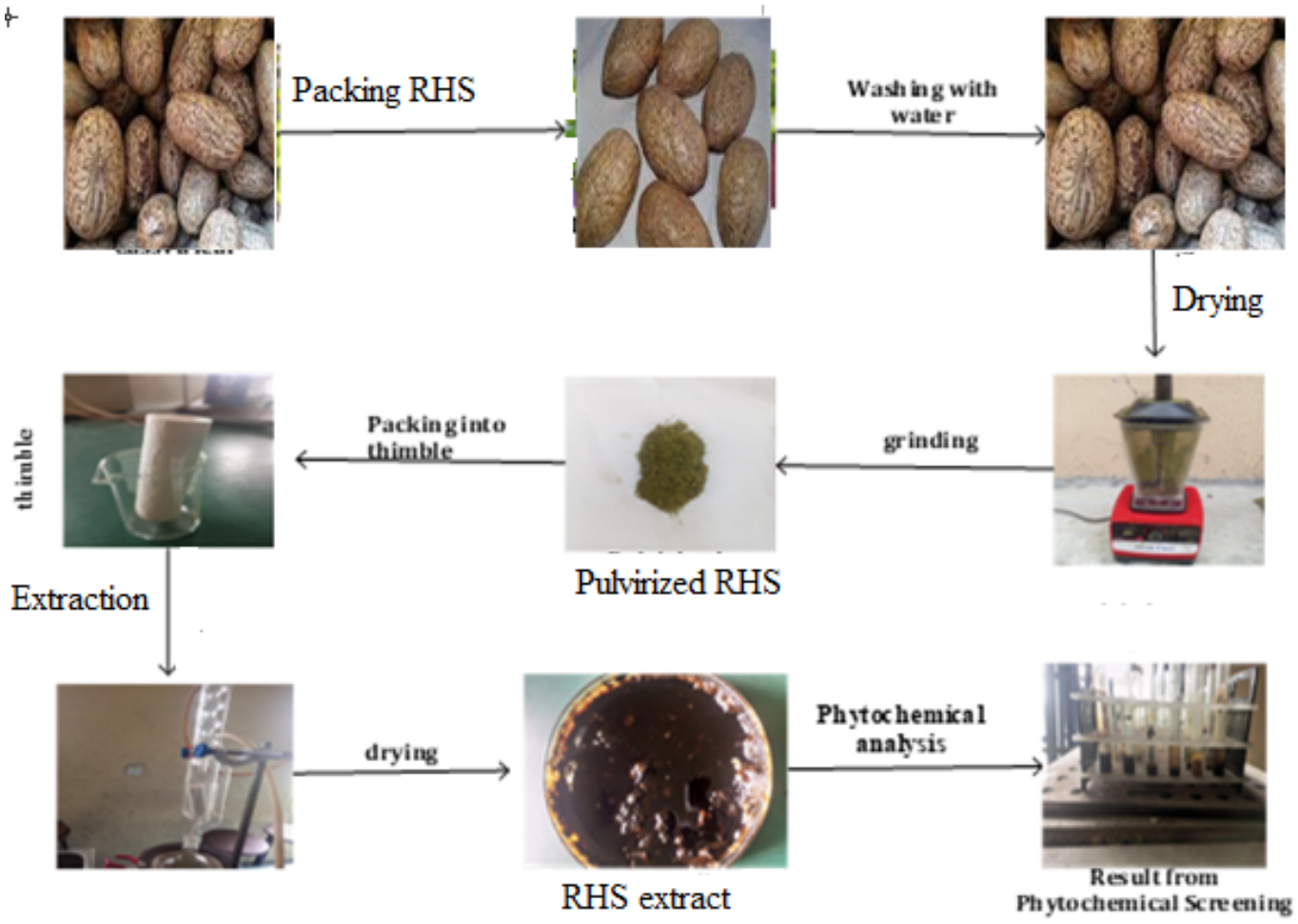

Figure 1. Flow diagram for the extraction and phytochemical screening of *Raphia hookeri* seed.

3.2.1. UV-visible spectrophotometry

The initial instrumental method used to monitor the development of nanoparticle production is often UV-Vis spectroscopy. This is because it clarifies important information about how nanoparticles are formed. A Perkin Elmer Lambda 40 UV-visible spectrometer was used to monitor the synthesis and progress of the manganese dioxide nanoparticles.

4 showed the UV-visible spectrum result for Manganese dioxide nanoparticles (MnO_2NP) respectively with maximum absorbance observed at 421 nm. This gives excellent agreement with those in literatures previously reported by Harish and Poonam [16] in their findings of the synthesis of MnO_2NPs. Aqueous extract of *Raphia hookeri* seed has helped in the reduction of the manganese acetate precursor which changed the colour of the MnO_2NP to black Hairui *et al.* [17]. Further, The UV-Vis absorbance spectrum of the MnO_2NPs looks has a well-defined peak at 421nm This is due the electronic transitions in MnO_2. This peak may be employed for the evaluation of the optical band gap of the MnO_2 nanoparticle as energy of the absorbed photons can be expressed in equation 2. The optical band gap energy value of 2.95 eV obtained is a characteristic for MnO_2 and speaks about its possible application in electronics and optoelectronics as sensors or photovoltaic materials Harish and Poonam [16].

$$E = \frac{hc}{\lambda}, \tag{2}$$

$$E = \frac{6.626\ x\ 10^{-34}\ x\ 3.00\ x\ 10^{8}}{421\ x\ 10^{-9}} = 4.72\ x\ 10^{-19} J = 2.95 eV. \tag{3}$$

3.2.2. Fourial Transform Infrared (FTIR)

The chemical properties, reactivity and bonding activities of the biosynthesized nanoparticles of MnO_2NP is revealed in Figure 5, which determined the presence of the functional groups on the nanoparticles surface. The FTIR spectrophotometry of model Nicolet iS10 FT-IR Spectrometer is used for this analysis which range from 4000 to 450 wave number (cm^{-1}). The absorption bands at 515.00 cm^{-1} and 480.00 cm^{-1} correspond to the bond of manganese oxide (Mn–O) [18, 19]. Thus, we concluded that the synthesized material is manganese oxide nanomaterial. Weak absorption peak found at 1700.00 cm^{-1} could be from -C=O stretching vibration of the carbonyl group

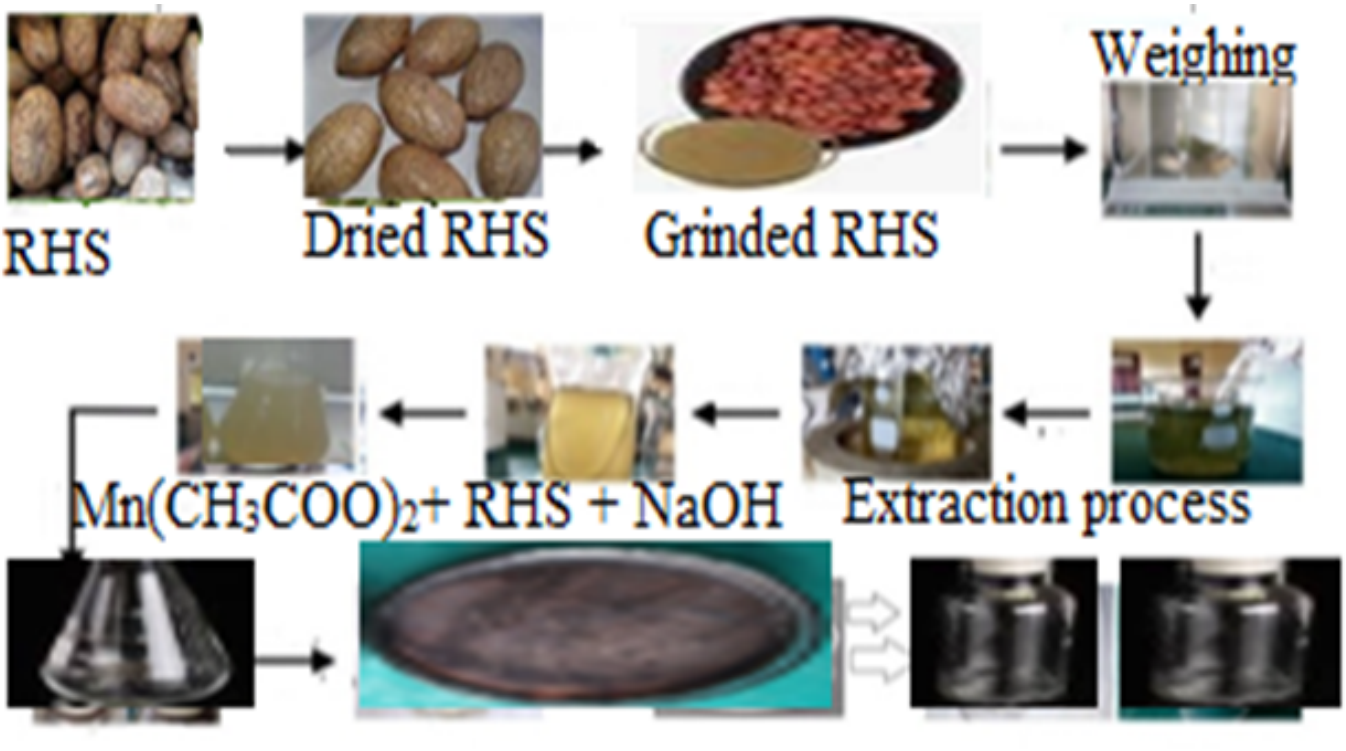

Figure 2. Flow diagram for the preparation of *Raphia hookeri* seed extract and synthesis of MnO_2NPs.

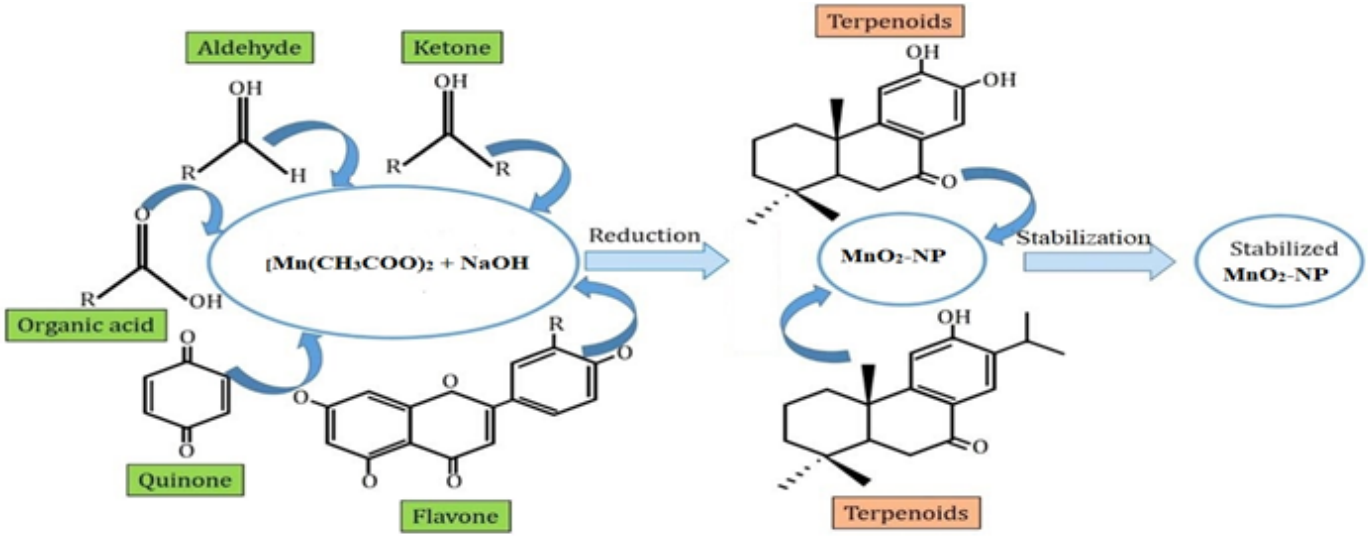

Figure 3. Mechanism of bio-reduction and stabilization of MnO_2-NPs using *Raphia hookeri* seed.

which could have formed a bond with the MnO_2NP from the flavonoids of the R.H.S. The weak band implies that there is probably a less density of carbonyl group or there could be a strong hydrogen bonding. The absorption peak at 3348.30 cm^{-1} can be linked to the hydroxide (-OH) stretching vibration. These functional groups found have high electron density and can help the nanoparticle adsorption processes to capture molecule.

3.2.3. *Scanning Electron Microscopy (SEM)*

The SEM is a highly specialized instrument that captures images of a specific sample by utilizing a focused electron beam to scan its surface. This process results in electron interaction with the atoms within the sample, which generates a diverse array of signals that ultimately produce micrographs or pictures containing valuable information regarding the composition and topography of the sample's surface. Figure 6 depicts the SEM micrographs of the MnO_2NP. The fundamental objective of the

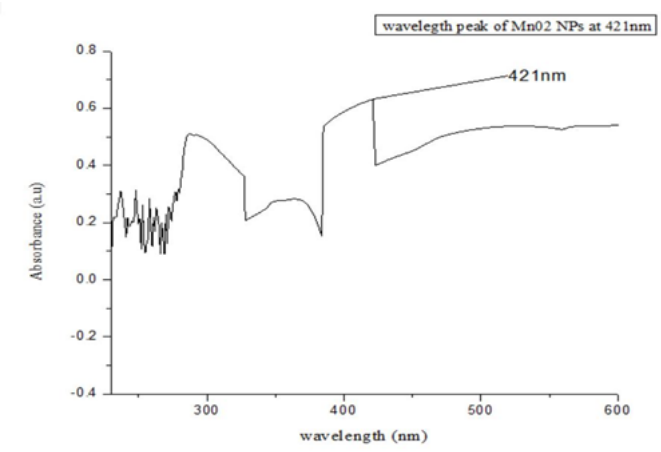

Figure 4. UV-Visible spectrum for MnO_2NP.

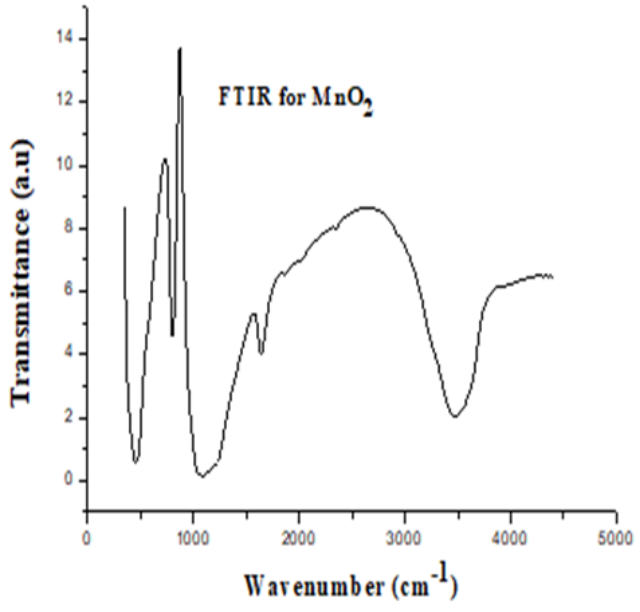

Figure 5. FTIR spectrum for MnO_2NP.

SEM is to reveal the surface structure and actual morphology of the MnO_2NP having rough and irregular shape, porosity and compact structure. The porous surface seen in the micrograph gives an idea of the presence of active sites which could be applied in different fields of study. Similar view was shared by Harish and Poonam [16] in the synthesis of nanoparticles of manganese oxide.

3.2.4. Transmission Electron Microscope (TEM)

The average particle size of the biosynthesized nanoparticles of MnO_2NP was achieved by using a TEM model JEOL2100 instrument, imageJ and origin lab software. Figure 7 showed the micrograph of MnO_2NP. These nanoparticles look to be well dispersed and there is some coalescing of the particles though this seems more evident with the formation of the clusters made of smaller particles. This points to the size

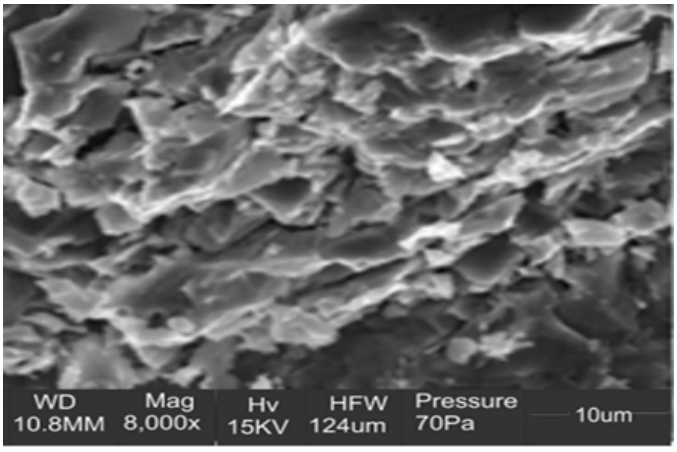

Figure 6. SEM micrograph of MnO_2NP.

distribution indicating that they were relatively small and this is very important in situations where uniformity in the characteristics of the particle is important such as in catalysis, electronics or in pharmaceuticals where they may be used for drug delivery systems. The scale bar of 100 nm helps to visualize the size of the particles provided next to it and indicates that they are indeed nanoparticles. Since there is little overlapping of the images of the particles and their clear contours are seen, it points to high-resolution imaging, which is characteristic of the TEM that gives structural and morphological information of specimens at an atomic level. Such size and distribution of the particles help in the growth mechanism to be founded and also in the possibility of adjusting the properties of the material for certain uses. The particle size of the nanoparticles showed that it has a very high surface area which explains its wide applications in adsorption studies Prabhat *et al.* [20].

3.2.5. Energy Dispersive X-ray analysis (EDX)

EDS analysis is one of the most popular methods on identification of components of biosynthesized MnO_2NPs. The result gave veritable information on the weight percentages of different elemental constituents in the biosynthesized MnO_2NPs. Figure 8 revealed the spectrum for MnO_2NPs. Result obtained showed that the EDX revealed the elements that make up the biosynthesized MnO_2NPs in their percentages and optical potential, which are manganese (70.96 %, 3.82 keV), Oxygen (25.67 %, 1.190 keV) and Carbon (8.34 %, 1.377 keV). This high percentage implies that the sample is probably a manganese compound or an alloy, this is supported by the XRD pattern of various manganese oxide and compounds. Since oxygen is present, the manganese may be present in an oxidized state with an oxide such as MnO_2.The presence of carbon in the nanoparticles is believed to have emerged from the *Raphia hookeri* seed.

3.2.6. Powdered X-ray Diffraction techniques (PXRD)

The Powdered X-ray diffraction (PXRD) technique is commonly used to determine the state of crystallinity and non-crystallinity of the biosynthesized nanoparticles with diffraction peaks. By examining these characteristics of the XRD

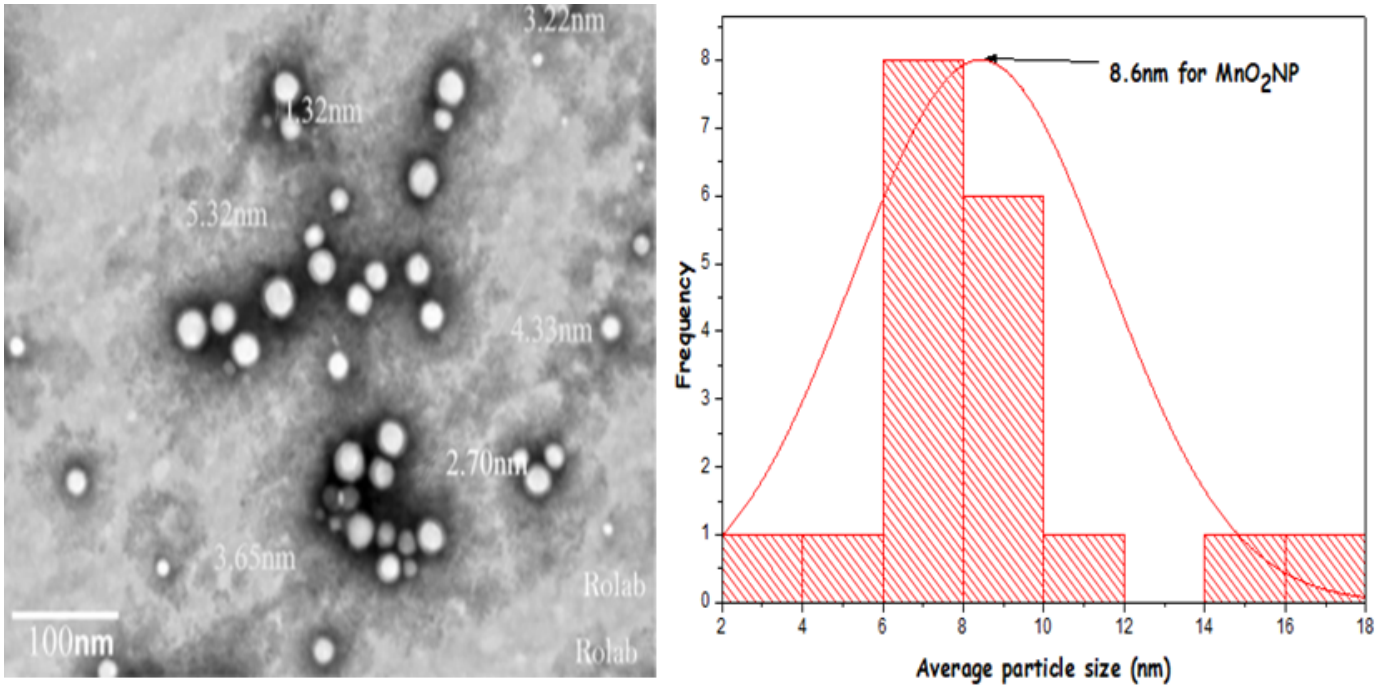

Figure 7. TEM micrograph of MnO_2NP.

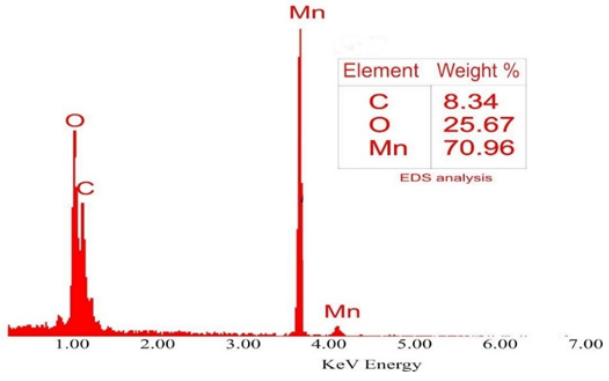

Figure 8. EDX micrograph of MnO_2NP.

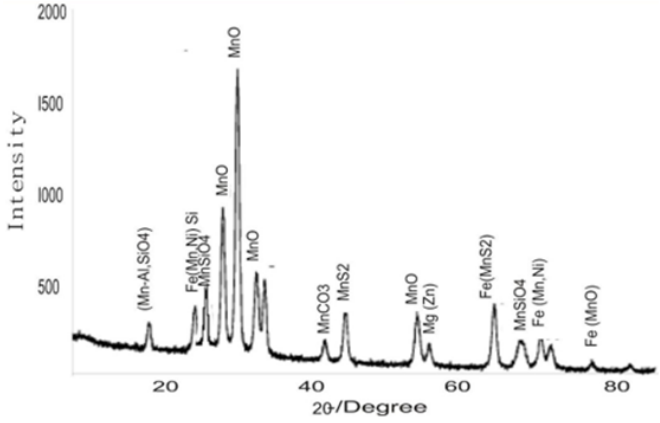

Figure 9. XRD spectra of MnO_2NP.

peaks such as peak sharpness, number of peaks, intensity, positions, and spacing, the state of crystallinity of the synthesized nanoparticles can assessed. Crystalline materials typically exhibit well-defined, sharp peaks with multiple distinct peaks and high intensity, indicating a higher degree of crystallinity. In contrast, amorphous materials with lower crystallinity may exhibit broad or diffuse peaks with lower intensity. Figure 9 showed the XRD spectrum with diffraction peaks for MnO_2NP seen at 2θ = 12.4, 21.6, 24.7, 31.2, 37.7, 40.5, 47.3, 54.3, 57.1 and 65.7 which are assigned to the (110), (200), (220), (310), (211), (301), (411), (600), (521) and (002) plane of MnO_2 respectively. The diffraction positions match the file well with JCPDS44-0141. According to obtained pattern, the manganese dioxide nanoparticles is a crystalline substance. This result is similar to past work of Prabhat *et al.* [21].

4. Conclusion

In this study, a nanoparticle of MnO_2NP was biosynthesized using an agricultural waste of *Raphia hookeri* seed as bioreductant. Extraction and phytochemical screening was experimented on the *Raphia hookeri* seed using water as an extractant. The phytochemical screening of the aqueous extract revealed the presence of phytochemicals that assisted in the biosynthesis of the MnO_2NPs. The MnO_2NP was biosynthesized using the bottom-up approach and the end product was described. The nature and characteristics of the biosynthesized MnO_2NP were revealed and several instrument methods employed, which included UV-visible spectrophotometer, FTIR, SEM, TEM, EDX, and XRD. This method provided the nanoparticles' structures, optical properties, porosity, crystallinity, and particle di-

ameter. These properties revealed the successful completion of the MnO_2NP and the potentiation of *Raphia hookeri* as a waste material for the formation of MnO_2NPs.

References

[1] M. J. Haque, M. M. Bellah, M. R Hassan & S. Rahman, "Synthesis of ZnO nanoparticles by two different methods and comparison of their structural, antibacterial, photocatalytic and optical properties", Nano Express **1** (2020) 010007. https://doi.org/10.1088/2632-959x/ab7a43.

[2] E. E. Elemike, D. C. Onwudiwe & J. I. Mbonu, "Facile synthesis of cellulose–ZnO-hybrid nanocomposite using Hibiscus rosa-sinensis leaf extract and their antibacterial activities", Applied Nanoscience **11** (2021) 1349. https://doi.org/10.1007/s13204-021-01774-y.

[3] K. Brindhadevi, S. Vasantharaj, S. Devanesan, L. Xinghui & F. Karim, "Fabrication and characterization of manganese dioxide (MnO_2) nanoparticles and its degradation potential of benzene and pyrene", Chemosphere **343** (2023) 140123. https://doi.org/10.1016/j.chemosphere.2023.140123.

[4] T. M. Abelneh, "Biosynthesis of Manganese Dioxide Nanoparticles and Optimization of Reaction Variables", Journal of nanotechnology and nanomaterials **5** (2024) 31. https://doi.org/10.33696/Nanotechnol.5.052.

[5] N. Penghui, Z. Yu & X. Hengyi "Synthesis, applications, toxicity and toxicity mechanisms of silver nanoparticles: A review", Ecotoxicology and Environmental Safety **253** (2023) 114636. https://doi.org/10.1016/j.ecoenv.2023.114636.

[6] S. Ahmed, M. Ahmad, B. L. Swami & S. Ikram, "A review on plants extract mediated synthesis of silver nanoparticles for antimicrobial applications: A green expertise", Journal of Advanced Research **7** (2016) 17. https://doi.org/10.1016/j.jare.2015.02.007.

[7] R. L. Thimappa, K. K. Naveen, M. Venkataramana, D. M Chakrabhavi, R. Shobith, D. P. Bangari, S. A. Bagepalli, H. Abeer, A. Abdulaziz, A. M. Jahangir, F. A. Elsayed, K. G. Vijai, N. S. Chandra & R. N. Siddapura, "Biofabrication of Zinc Oxide Nanoparticles With Syzygium aromaticum Flower Buds Extract and Finding Its Novel Application in Controlling the Growth and Mycotoxins of Fusarium graminearum", Frontiers in microbiology **10** (2019) 1244. https://doi.org/10.3389/fmicb.2019.01244.

[8] H. Amir, H. Muhammad, U.K. Sana, K. Istikhar, A. Muhammad, & A. Naveed, "Lathyrus aphaca Extract MnO Nanoparticles: Synthesis, Characterization, and Photocatalytic Degradation of Methylene Blue Dye", Photocatalysis: Research and Potential **3** (2024) 10004. https://doi.org/10.35534/prp.2024.10004.

[9] S. Ghosh, P. More, R. Nitnavare, S. Jagtap, R. Chippalkatti, A. Derle, R. Kitture, A. Asok & S. Kale, "Dioscorea bulbifera mediated synthesis of novel Au core Ag shell nanoparticles with potent antibiofilm and antileishmanial activity", Journal of Nanobiotechnology **10** (2012) 1. https://onlinelibrary.wiley.com/doi/10.1155/2015/562938.

[10] V. Sekar, M. Balasubramanian, R. Palaniappan & V. Baskaralingam, "Assessment of biopolymer stabilized silver nanoparticle for their ecotoxicity on Ceriodaphnia cornuta and antibiofilm activity", Journal of Environmental Chemical Engineering **4** (2016) 2076. https://doi.org/10.1016/j.jece.2016.03.036.

[11] H. Mohammad, A. H. Hasan & E. Behrouz, "Fabrication of Manganese Dioxide Nanoparticles in Starch and Gelatin Beds: Investigation of Photocatalytic Activity", Chemical Methodologies **8** (2024) 37. https://doi.org/10.48309/chemm.2022.424921.1739.

[12] P. A. Oluyori, A. O. Dada & A. A. Inyinbor, "Phytochemical Analysis and Antioxidant Potential of Raphia hookeri leaf and Epicarp", Oriental Journal of Chemistry **34** (2018) 6. http://dx.doi.org/10.13005/ojc/340608.

[13] A. O. Okewale & B. H. Akpeji, "Green synthesis of zinc oxide nanoparticles (ZnONPs) from cassava leaf (Manihot esculenta) and its application as a corrosion inhibitor formild steel in 1M hydrochloric acid", Journal of Engineering, Science, and Technology **6** (2022) 2714. https://www.researchgate.net/publication/373237707_APWEN_JOURNAL_VOLUME_6_ISSUE_1_1.

[14] L. Haibin, Z. Xueyang, A. K. Shakeel, L. Wenqiang & W. Lei, "Biogenic Synthesis of MnO2 Nanoparticles With Leaf Extract of Viola betonicifolia for Enhanced Antioxidant, Antimicrobial, Cytotoxic, and Biocompatible Applications", Frontiers in microbiology **12** (2021) 761084. https://doi.org/10.3389/fmicb.2021.761084.

[15] M. A. Samy, A. A. Moustafa, E. H. Elsayed, I. R. Entsar & D. G. Aseel "Biosynthesis and Characterization of Silver Nanoparticles Produced by Plant Extracts and Its Antimicrobial Activity", South Asian Journal of Research in Microbiology **3** (2019) 1. https://doi.org/10.9734/sajrm/2019/v3i130077.

[16] K. M Harish & S. Poonam, "Synthesis and Characterization of MnO_2 Nanoparticles using Co-precipitation Technique", International Journal of Chemistry and Chemical Engineering **3** (2013) 155. https://www.ripublication.com/ijcce_spl/ijccev3n3spl_05.pdf.

[17] L. Hairui, K. Peipei, L. Ying, A. Yifan, H. Yanting, J. Xiyuan, C. Xin, Q. Yunfei, T. Ramesh & W. Xiao, "Zinc oxide nanoparticles synthesized from the *Vernonia amygdaline* shows the anti-inflammatory and antinociceptive activities in the mice model", Artificial Cells, Nanomedicine and Biotechnology **48** (2020) 1068. https://doi.org/10.1080/21691401.2020.1809440.

[18] L. Li, Y. Pan, L. Chen & G. Li, "One-dimensional α-MnO_2: trapping chemistry of tunnel structures, structural stability, and magnetic transitions", Solid State Chem. **180** (2007) 2896. doi.org/10.1016/j.jssc.2007.08.017

[19] L. Kang, M. Zhang, Z. H. Liu & K. Ooi, "IR spectra of manganese oxides with either layered or tunnel structures", Spectrochim Acta A Mol Biomol Spectrosc **67** (2007) 864. https://doi.org/10.1016/j.saa.2006.09.001.

[20] P. G. Tratnyek & R. L. Johnson, "Nanotechnologies for environmental cleanup", Nano today **1** (2006) 44. http://dx.doi.org/10.1016/S1748-0132(06)70048-2.

[21] K. Prabhat, K. Jaspinder & K. T. Anurag, "Synthesis and Characterization of Manganese dioxide Agglomerated Nanoparticles for Supercapacitor Application", International Conference on Materials Science and Engineering **1248** (2022) 012052. doi.org/10.1088/1757-899X/1248/1/012052.